

Aberystwyth University

Instabilities in two-dimensional flower and chain clusters of bubbles

Fortes, M. A.; Vaz, M. Fatima; Cox, Simon; Teixeira, Paulo

Published in:

Colloids and Surfaces A: Physicochemical and Engineering Aspects

DOI:

[10.1016/j.colsurfa.2007.02.039](https://doi.org/10.1016/j.colsurfa.2007.02.039)

Publication date:

2007

Citation for published version (APA):

Fortes, M. A., Vaz, M. F., Cox, S., & Teixeira, P. (2007). Instabilities in two-dimensional flower and chain clusters of bubbles. *Colloids and Surfaces A: Physicochemical and Engineering Aspects*, 309(1-3), 64-70.
<https://doi.org/10.1016/j.colsurfa.2007.02.039>

General rights

Copyright and moral rights for the publications made accessible in the Aberystwyth Research Portal (the Institutional Repository) are retained by the authors and/or other copyright owners and it is a condition of accessing publications that users recognise and abide by the legal requirements associated with these rights.

- Users may download and print one copy of any publication from the Aberystwyth Research Portal for the purpose of private study or research.
- You may not further distribute the material or use it for any profit-making activity or commercial gain
- You may freely distribute the URL identifying the publication in the Aberystwyth Research Portal

Take down policy

If you believe that this document breaches copyright please contact us providing details, and we will remove access to the work immediately and investigate your claim.

tel: +44 1970 62 2400
email: is@aber.ac.uk

Instabilities in two-dimensional flower and chain clusters of bubbles

M. A. Fortes¹, M. Fátima Vaz^{1*}, S. J. Cox² and P.I.C. Teixeira^{3‡}

¹Instituto de Ciência e Engenharia de Materiais e Superfícies and
Departamento de Engenharia de Materiais Instituto Superior Técnico,
Technical University of Lisbon,

Av. Rovisco Pais, 1049-001 Lisbon, Portugal

²Institute of Mathematical and Physical Sciences, University of Wales,
Aberystwyth, Ceredigion SY23 3BZ, UK

³Faculdade de Engenharia, Universidade Católica Portuguesa, Estrada de Talaíde, P-2635-
631 Rio de Mouro, Portugal

[‡]Present address - Instituto Superior de Engenharia de Lisboa, Rua Conselheiro Emídio
Navarro 1, 1950-062 Lisboa, and Centro de Física Teórica e Computacional, Universidade
de Lisboa, Avenida Professor Gama Pinto 2, 1649-003 Lisboa, Portugal

*corresponding author - fatima.vaz@ist.utl.pt; fax: 351218418132

Abstract

We assess the stability of simple two-dimensional clusters of bubbles relative to small displacements of the vertices, at fixed bubble areas. The clusters analysed are: 1) flower clusters consisting of a central bubble of area λ surrounded by N shells each containing n bubbles of unit area, 2) periodic chain clusters consisting of N "parallel" rows of n bubbles of unit area and width w . The energy and bubble pressures of the symmetrical, unbuckled clusters are found analytically as a function of λ and w for given N and n . Both types of clusters studied show a single energy minimum at a critical λ_m or w_m . At the energy minimum for flower clusters, the pressure in the central bubble vanishes. The clusters show a symmetry-breaking buckling instability under compression at a critical λ_b or w_b . The corresponding critical energy E_b was determined with the Surface Evolver software. While for $N=1$ the conditions $\lambda_b = \lambda_m$, $w_b = w_m$ and $E_b = E_m$ hold, for $N>1$ buckling requires further compression beyond the minimum, for which the energy increases with increasing compression (decreasing λ or w), and the excess pressure in the central bubble of the flower clusters becomes negative.

Keywords: Instabilities, clusters, Surface Evolver, bubbles, foams

1. Introduction

Considerable attention has been given in recent years to the determination of the perimeter minima of finite and periodic two-dimensional (2D) clusters with given cell areas. In 2001 Hales [1] proved the honeycomb conjecture, which states that the partition of the plane into regular hexagons of equal area has least perimeter. Clusters have been examined analytically [2-8], numerically [9-11] and experimentally [7].

Perimeter-minimising clusters have a simple analogy in the structure of a dry 2D foam [12]. The surface energy of a 2D foam is its perimeter multiplied by the film energy per unit length or film tension γ . We therefore identify cells with bubbles and perimeter with energy. Minimisation of surface energy implies Plateau's rules for equilibrium [13, 14]: the films are circular and meet at angles of $2\pi/3$ at trivalent vertices. The contractile tendency of a film, endowed with the film tension γ , is balanced by a pressure difference across it; the Laplace law dictates that a film of radius of curvature R is balanced by a pressure difference $\Delta p = \gamma/R$.

In this paper we discuss the stability of the equilibria of two types of 2D finite clusters of bubbles: 1) flower clusters with N shells, each with n bubbles (“petals”) of the same area $A=1$, surrounding a central bubble of area λ ; 2) chain clusters with N rows, each containing n bubbles of unit area, periodic in one direction (period nw , where w is the width of a bubble). Examples are shown in Fig. 1. Two-dimensional clusters of both types with $N=1$ were previously discussed in the literature [7, 10, 11, 15]. Here, we extend the work to higher N .

The flower clusters for $N=1$ were shown [11] to exhibit a buckling type of instability for $n>6$ when the area ratio λ is reduced to a critical value λ_m , at which point the cluster energy attains a minimum E_m as a function of λ (i.e. $\lambda_m = \lambda_b$) as shown in Fig.2 (see Appendix A). At this critical point the energy per petal E_m/n was found to be independent of n . The cluster becomes “floppy” and destabilises, losing its n -fold symmetry. The energy E_b of the buckled clusters with $\lambda < \lambda_m$ remains constant, $E = E_m$ [11], see Fig. 2. The pressure in the central bubble is equal to the outside pressure (excess pressure $p^*=0$) at the energy minimum [16], and p^* decreases to negative values with increasing compression (decreasing λ). The buckling instability in flower clusters with $N=1$ was analysed by Weaire *et al.* [11] with the Surface Evolver program [17], which allows the calculation of the Hessian matrix (the matrix of second derivatives) of the energy relative to infinitesimal displacements of the vertices, at constant bubble areas. The instability occurs when one of the eigenvalues of the Hessian becomes zero and buckling is evident in the distortion of the central bubble. The fundamental eigenmode causes an elliptical buckling of the cluster. These buckled configurations determined with the Surface Evolver were not observed experimentally [18, 19]. Instead, another type of instability was detected in which a bubble is ejected from the ring of “petals” [18, 19]. The difference between experiment and simulation can be attributed to liquid held between the bubbles (Plateau borders) in the experiment and not present in the simulations.

Brakke [20] provided one example of a flower cluster with $N=2$, $n=24$ and examples of chain clusters with N up to 64 and $n=2$, which, under the Hessian matrix method, are stable at the energy minimum. Thus the energy minimum does not provide an indication of the point at which the instability will occur, and the Hessian eigenvalues must instead be calculated. For example, the flower cluster with $N=2$, $n=24$, has $\lambda_m=14.939$ but becomes

unstable at $\lambda_b = 13.084$, when the excess pressure in the central bubble is $p_b^* = -0.068$. In this paper we show that, for any $N > 1$, p_b^* is negative.

In periodic chain clusters with $N=1$, buckling occurs at the energy minimum as a function of the width per bubble, w , at which point the straight inter-bubble films start to rotate [15]. The buckled configuration can be calculated analytically. It has the energy of the minimum ($E_b = E_m$) and the $E(w)$ plot is as in Fig. 2, i.e. similar to that for $N=1$ flower clusters. Our Surface Evolver calculations confirm that $w_m = w_b$ for $N=1$, but not for $N > 1$. For example, for $N=2$, $n=24$, the minimum occurs at $w_m = 0.848$ but $w_b = 0.830$ (the excess pressure in the bubbles is $p_b^* = 1.204$ at buckling).

Here we determine the behaviour of both flower and chain clusters with multiple layers of bubbles ($N > 1$), and compare it with the $N=1$ case. We will show, using analytical and Surface Evolver calculations, that the special properties of clusters with $N=1$, reviewed above, do not apply when $N > 1$.

2. Analytical solutions

The Plateau rules [13, 14] enable the analytical determination of the equilibrium configuration of a cluster of bubbles. For unbuckled flower clusters, the energy E as a function of λ for fixed n and N is shown in Fig. 3a (details are given in Appendix A). The area ratio λ_m at which the minimum occurs is given in Fig. 3b and in Fig. 3c we plot the energy per petal at the minimum $E_m/\gamma N$. It was shown by Teixeira and Fortes [16] that the excess pressure p^* in the central bubble vanishes at the energy minimum with respect to λ , for any n and N .

The results of calculations for chain clusters (details are given in Appendix B) are shown in Fig. 4: the width per bubble w_m and the energy $E_m/\gamma N$ per bubble at the energy minimum as a function of N .

3. Surface Evolver results

3.1 Flower clusters

We used the Surface Evolver [17] in circular arc mode to determine the energy of a cluster, which provides a check on the calculated energy $E(\lambda)$ and allows us to find the point of instability of a flower cluster with the Hessian. Each film is represented by a circular arc, making the calculations precise and fast.

The critical values λ_b at which zero eigenvalues first appear and the cluster becomes unstable under compression were determined for clusters with $N=1$, $N=2$ and $N=4$ and a range of values of n . As mentioned above, the critical area for buckling, λ_b , for $N=1$ coincides with that at the energy minimum, λ_m , at which point the excess pressure in the central bubble p^* vanishes. However, for $N > 1$ we always found that $\lambda_b < \lambda_m$ and $p_b^* < 0$ as in the example of Brakke for $N=2$ [20].

For $N > 1$, symmetry breaking instabilities in flower clusters thus occur when $p^* < 0$ and $dE/d\lambda < 0$ and in general lead to a distorted, elliptical central bubble (as for $N=1$) as shown in Fig 5a for $N=2$ and $n=12$ and in Fig. 5b for $N=4$ and $n=12$. The energy of the distorted cluster increases with decreasing λ , and is only very slightly lower than, by

around 0.01%, the energy that a symmetrical cluster with the same λ would have (see Fig 5c and 5d), in contrast with what happens for $N=1$ (see Fig.2) as discussed above.

In Fig. 6a, b we show λ_b and λ_m for flower clusters with N between 1 and 5 and in Fig. 6c the ratio λ_b / λ_m . The excess pressure in the central bubble, p_b^* , at buckling is shown in Fig. 6d. We were not able to find simple relationships between λ_b and the energy per petal bubble E_b/nN or the excess pressure p^* in the central bubble at buckling. It is striking that the λ_b / λ_m and p_b^* plots of Fig. 6c and d are similar. The p_b^* data of Fig. 6d seems to indicate that an increase in the bending stiffness of the clusters imparted by an increase in N does not in general occur.

Note that it is not possible to construct flower clusters for all choices of n , N and λ as we will discuss elsewhere. For example, for $N=4$, $n=9$ and λ in the interval $0.001 \leq \lambda \leq 4$ no clusters with 9-fold symmetry (i.e. the proper flower clusters) could be produced with the Surface Evolver. Other values for which no stable cluster could be found can be determined from the starting point of each curve in Fig. 6c or d.

3.2. Chain clusters

The Surface Evolver was used to examine chain clusters which are confined in a periodic box of length nw . Examples of the buckling instability in chain clusters with $N=1$, $N=2$ and $N=4$ are shown in Fig. 7.

As for flower clusters, buckling of chain clusters with $N=1$ occurs at the energy minimum, but for $N>1$ buckling occurs beyond the minimum, for $w_b < w_m$, i.e. when $dE/dw < 0$. For $N=1$ the energy of the buckled configuration is independent of w and equal to the minimum energy of the unbuckled configuration, as for flower clusters with $N=1$ (Fig. 2). For $N=1$, the energy of the buckled configuration can be analytically determined in 2D [15] and also in 3D chain clusters [21]. It is indeed independent of λ or w in their interval of existence. For $N>1$, however, the energy of the buckled configurations of the chains for $w < w_b$ is again close to, though slightly lower by around 0.005%, the calculated energy of the unbuckled configuration for the same w , as shown in Fig. 8.

The width of a bubble in a chain at the point of buckling w_b is plotted in Fig. 9a. It increases with n for $N>1$ (the corresponding width in an unstrained honeycomb is 1.075). Fig. 9b shows the energy per bubble at buckling E_b/nN (the value for the unstrained honeycomb is 1.861). Fig. 9c shows the ratio w_m/w_b . Finally, Fig 9d shows the excess pressure in the bubbles at buckling. In each case this pressure is above the excess pressure at the energy minimum. Again, w_m/w_b and p_b^* exhibit similar behaviour.

Summary

Our main objectives in this study were the assessment of the stability of simple 2D clusters (flower and chain clusters) and the determination of the distorted configurations that result from instabilities. Both flower and chain symmetrical clusters show an energy minimum under compression (i.e. decreasing the area of the central bubble in flower clusters or decreasing the width per bubble of the chain clusters). At the energy minimum the pressure in the central bubble of a flower cluster vanishes. However, the instability does not necessarily occur at the energy minimum, as conjectured by Vaz and Fortes [19]. Determination of the eigenvalues of the Hessian matrix shows that, except for $N=1$ (one

shell of bubbles in flower clusters and one row of bubbles in chain clusters), instability occurs beyond the energy minimum, in the region where the energy increases with compression and the excess pressure in the central bubble of flower clusters is negative. The distorted configurations predicted by the Surface Evolver have not yet been observed experimentally except for the chain clusters with $N=1$ [15]. The difficulty lies in performing either very "dry experiments" or simulations that include the liquid between the bubbles.

Acknowledgements

The authors thank Prof. Denis Weaire and Prof. K. Brakke for helpful discussions.

References

- [1] T. C. Hales, Discrete Comput. Geom., 25 (2001) 1.
- [2] J. Foisy, M. Alfaro, J. Brock, N. Hodges, J. Zimba and F. Morgan, Pac. J. Math., 159 (1993) 47.
- [3] F. Morgan, Geometric Measure Theory: A Beginner's Guide, MA: Academic, Boston, 2000.
- [4] W. Wichiramala, J. Reine. Angw. Math., 567 (2004) 1.
- [5] P.I.C. Teixeira, F. Graner and M. A. Fortes, Eur. Phys. J. E, 9 (2002) 161.
- [6] F. Morgan, Am. Math. Mon., 101 (2000) 343.
- [7] M. F. Vaz and M. A. Fortes, J. Phys. : Condens. Matter, 13 (2001) 1395.
- [8] P.I.C. Teixeira and M. A. Fortes, J. Phys. : Condens. Matter, 14 (2002) 5719.
- [9] S. J. Cox, F. Graner, M. Fátima Vaz, C. Monnereau-Pittet and N. Pittet, Phil. Mag., 11 (2003) 1393.
- [10] S. J. Cox and F. Graner, Phil. Mag., 83 (2003) 2573.
- [11] D. Weaire, S.J. Cox and F. Graner, Eur. Phys. J. E, 7 (2002) 123.
- [12] D. Weaire and S. Hutzler, The Physics of Foams, Oxford University Press, Oxford, 1999.
- [13] J.F.A. Plateau, Statique Expérimentale et Théorique des Liquides Soumis aux Seules Forces Moléculaires, Gauthier-Villard, Paris, 1873.
- [14] J.E. Taylor, Ann. Math., 103 (1976) 489.
- [15] M. A. Fortes, M. E. Rosa, M. F. Vaz and P. I. C. Teixeira, Eur. Phys. J. E, 15 (2004) 395.
- [16] P.I.C. Teixeira and M. A. Fortes, J. Phys. : Condens. Matter, 17 (2005) 2327.
- [17] K. Brakke, Exp. Math., 1 (1992) 141; <http://www.susqu.edu/brakke/evolver/evolver.html>
- [18] S.J.Cox, M. F. Vaz and D. Weaire, Eur. Phys. J. E., 11 (2003) 29
- [19] M. F. Vaz and M. A. Fortes, Eur. Phys. J. E., 11 (2003) 95.
- [20] K. Brakke, private communication;
<http://www.susqu.edu/brakke/evolver/evolver/examples/cluster/>.
- [21] S. Bohn, Eur. Phys. J. E, 11 (2003) 177.

Appendix A- Properties of symmetric flower clusters

For symmetrical unbuckled flower clusters the analytical calculations are not straightforward because there are curved inner films, although the films in the radial direction are straight by symmetry. The curved films have (positive) radii R_0, R_1, \dots, R_N where N is the number of layers. The layers are numbered $1, \dots, i, \dots, N$ starting in the innermost layer. The central bubble is bubble 0. For $n > 6$ the curvature of the films of the central bubble is opposite to that of the other films. It is convenient to consider the chords of the curved films. The angle between a film and its chord is θ_i ($i=1..N$), i.e. the subtended angle of the circular film is $2\theta_i$. The chord polygon of a bubble in layer i is shown in Fig. A1. Introducing the equilibrium condition that angles between points of films at a vertex must be $2\pi/3$:

$$\theta_0 = \frac{\pi}{6} - \frac{\pi}{n} ; \quad \theta_i = \frac{\pi}{2n} , \quad (1 \leq i \leq N-1); \quad \theta_N = \frac{\pi}{6} + \frac{\pi}{n} . \quad (A1)$$

The areas of the bubbles are expressed in terms of the chord lengths, $L_i = 2R_i \sin \theta_i$ and the angles θ_i and lead, upon considerable simplification, to the following equations for the R_i ($i=0..N$ with $N > 1$):

$$\begin{aligned} R_0^2 &= \frac{\lambda}{nc_0} ; \\ c_i R_i^2 &= c_0 R_0^2 + i , & (1 \leq i \leq N-1); \\ c_N R_N^2 &= c_0 R_0^2 + N \end{aligned} \quad (A2a)$$

with

$$\begin{aligned} c_0 &= -\theta_0 + \frac{1 \sin \theta_0}{2 \sin (\pi/n)} ; \\ c_i &= 2\theta_i - \frac{1}{2} \operatorname{tg} \theta_i , & (1 \leq i \leq N-1); \\ c_N &= \theta_N + \frac{1 \sin \theta_N}{2 \sin (\pi/n)} . \end{aligned} \quad (A2b)$$

These equations give the R_i ($i=0..N$) for each λ , N and n .

The excess pressure in the central bubble, p^* , is given by

$$\frac{p^*}{\gamma} = -\frac{1}{R_0} + \sum_{i=1}^N \frac{1}{R_i} \quad (A3)$$

and the energy is

$$\frac{E}{2n\gamma} = -c_0 R_0 + \sum_{i=1}^{N-1} c_i R_i + c_N R_N . \quad (A4)$$

Both depend on N, n and λ .

At the energy minimum $dE=0$ we have

$$-c_0 dR_0 + c_1 \sum_{i=1}^{N-1} dR_i + c_N dR_N = 0 . \quad (\text{A5})$$

Differentiation of equation (A2a) at fixed n, N , gives

$$c_0 R_0 dR_0 = c_1 R_i dR_i = c_N R_N dR_N \quad (1 \leq i \leq N-1). \quad (\text{A6})$$

Combining equation (A5) and (A6) with (A3) we find

$$p^*=0 \quad (\text{A7})$$

at the energy minima. (This is in fact a general property of free bubble clusters [16]).

For clusters with a single layer ($N=1$), we have

$$\theta_0 = \frac{\pi}{6} - \frac{\pi}{n} ; \quad (\text{A8})$$

$$\theta_1 = \frac{\pi}{6} + \frac{\pi}{n} ;$$

$$c_0 = -\theta_0 + \frac{1}{2} \frac{\sin \theta_0}{\sin(\pi/n)} ; \quad c_1 = \theta_1 + \frac{1}{2} \frac{\sin \theta_1}{\sin(\pi/n)} ; \quad (\text{A9})$$

$$R_0^2 = \frac{\lambda}{nc_0} ; \quad c_1 R_1^2 = c_0 R_0^2 + 1 ; \quad (\text{A10})$$

$$\frac{E}{2n\gamma} = -c_0 R_0 + c_1 R_1 ; \quad \frac{p_0}{\gamma} = -\frac{1}{R_0} + \frac{1}{R_1} . \quad (\text{A11})$$

At the energy minimum $p^*=0$ and $R_0=R_1=R$. From equation (A2a) we find $(c_1 - c_0)R^2 = 1$

and $\lambda = \frac{nc_0}{(c_1 - c_0)^{1/2}}$. For $N=1$ the energy per petal at the energy minimum $E_m/(n\gamma)$ is

$$\frac{E_m}{n\gamma} = 2(c_1 - c_0)^{1/2} = 2\left(\frac{\pi}{3} + \frac{\sqrt{3}}{2}\right)^{1/2} = 2.7662 ,$$

(A12)

independent of n (cf. Fig. 5d).

Appendix B- Properties of symmetric chain clusters

In unbuckled chain clusters with any N , n , the inner edges are straight because of the Plateau law of angles of 120° at vertices. The pressure is thus uniform but larger than the outside pressure, because the peripheral films are curved (Fig. 1). Let w be the width of one cell, and R_0 the radius of the peripheral films. We have $R_0 = w$. Denoting by L_1 the length of the straight films in the peripheral cells, and by L_2 the length of inner films, both perpendicular to the chain direction, and noting that the length of the inner inclined films is $w/\sqrt{3}$ we obtain for the area of a peripheral cell

$$A_p = wL_1 + w^2 \left(\frac{\pi}{6} - \frac{\sqrt{3}}{6} \right) \quad (\text{B1})$$

and for the area of an inner cell

$$A_i = wL_2 + \frac{w^2}{2\sqrt{3}}. \quad (\text{B2})$$

Setting $A_p = A_i = 1$ we obtain L_1 and L_2 as a function of w .

The total energy is

$$\frac{E}{\gamma} = n \left[\frac{2\pi}{3} w + 2L_1 + (N-2)L_2 + \frac{2w}{\sqrt{3}}(N-1) \right]. \quad (\text{B3})$$

Introducing the relations between L_1 , L_2 and w yields

$$\frac{E}{\gamma nN} = \frac{1}{w} + w \left(\frac{\sqrt{3}}{2} + \frac{\pi}{3N} \right). \quad (\text{B4})$$

There is an energy minimum at

$$w_m = \left(\frac{\sqrt{3}}{2} + \frac{\pi}{3N} \right)^{-1/2}; \quad (\text{B5})$$

$$\frac{E_m}{\gamma nN} = 2 \left(\frac{\sqrt{3}}{2} + \frac{\pi}{3N} \right)^{1/2}. \quad (\text{B6})$$

The excess pressure in the bubbles is $p^* = \gamma/w$. The width w_m for $N=1$ is $\left(\frac{\sqrt{3}}{2} + \frac{\pi}{3} \right)^{-1/2}$; for chains (with $N=1$) of disks or of regular hexagons in contact, the values of w are, respectively, 1.128 and 1.074.

Figure Captions

Figure 1 – Flower clusters with (a) $N=2$ and $n=12$; (b) $N=4$ and $n=12$. The central bubble has area λ , while the “petals” have unit area; (c) Chain cluster with $N=4$ and $n=30$. The width of a bubble is w . Only the peripheral edges are curved, with radius R_0 and subtended angle $2\theta_0$, where θ_0 is the angle between the curved films and their chords.

Figure 2 - Schematic representation of the energy as a function of w or λ for $N=1$ in flower and chain clusters. The short horizontal segment illustrates that for the buckled clusters, only in the case $N=1$, the energy remains constant. Actual values are different for flower and chain clusters (see text).

Figure 3- Plots of the exact relations derived in Appendix A for symmetrical flower clusters with N shells, each with n petals ($n>6$) of unit area surrounding a central bubble of area λ : a) energy per petal bubble $E/n\gamma$ versus λ for $N=2$ and $n=12$; b) area λ_m at energy minimum versus n for various N ; c) energy minimum per petal, $E_m/nN\gamma$ versus n for various N . Some of these clusters can not be constructed.

Figure 4 - Bubble width and energy per bubble at the energy minimum as a function of the number of rows N in chain clusters.

Figure 5 - Buckled flower clusters: (a) $N=2$ and $n=12$ for $\lambda=1$. In this cluster $\lambda_m=1.40$ and $\lambda_b=1.11$; (b) $N=4$ and $n=12$ for $\lambda=\lambda_b$. In this cluster $\lambda_m=0.98$ and $\lambda_b=0.89$; (c) and (d) Energy as a function of λ of the symmetrical configuration (exact calculations and Surface Evolver) and of the distorted (buckled) configuration, respectively for the clusters with $N=2$ and $n=12$ and for $N=4$ and $n=12$. For the same λ , the energies of the buckled and symmetrical clusters are almost the same.

Figure 6 – Surface Evolver results for flower clusters for various N and n : a) the area of the central bubble at the point of instability, λ_b ; b) the area at which the energy minimum occurs, λ_m ; c) the ratio λ_b/λ_m and d) the excess pressure p_b^* in the central bubble at the point of instability.

Figure 7 - Buckled configurations of chain clusters for a) $N=1$ and $n=3$; b) $N=2$ and $n=7$; c) $N=2$ and $n=15$ and d) $N=4$ and $n=20$.

Figure 8 –Energy per bubble as a function of width of the bubbles w for a chain cluster with $N=2$ and $n=20$. Here $w_m=0.848$ and $w_b=0.822$.

Figure 9 - Chain cluster results. a) Critical width w_b at which buckling occurs; b) Energy E/nN at the critical width; c) ratio w_m/w_b and d) excess bubble pressure at $w=w_b$.

Figure A1 – Definition of radii and angles of films in flower clusters. θ_i is one half of the subtended angle of a film of radius R_i , as in Fig. 1.

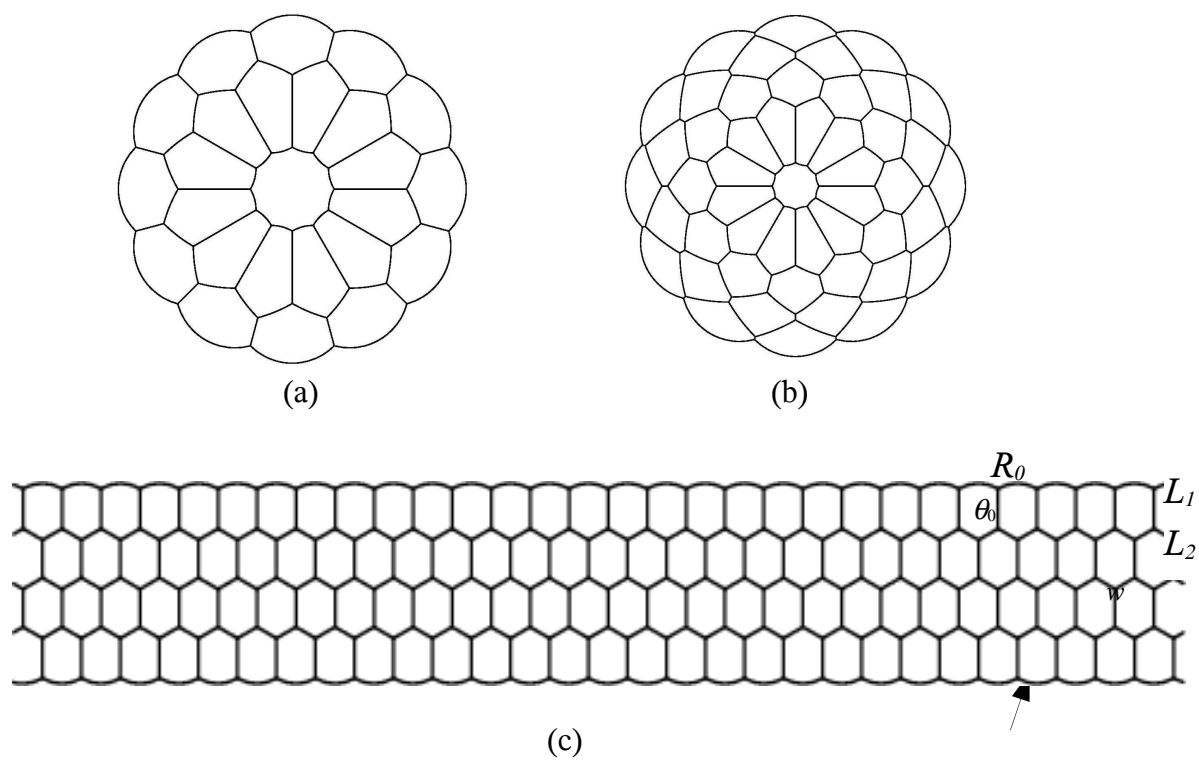


Figure 1

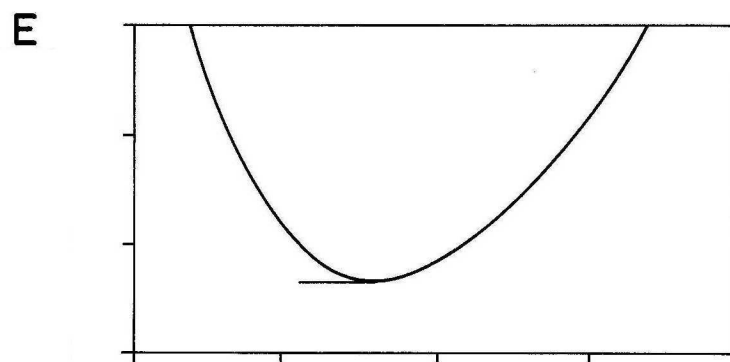


Figure 2

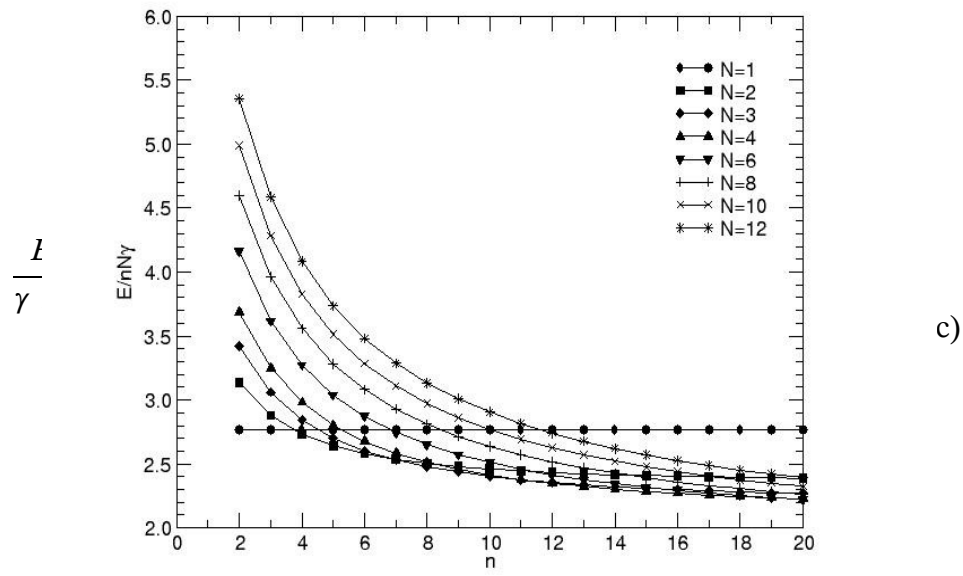
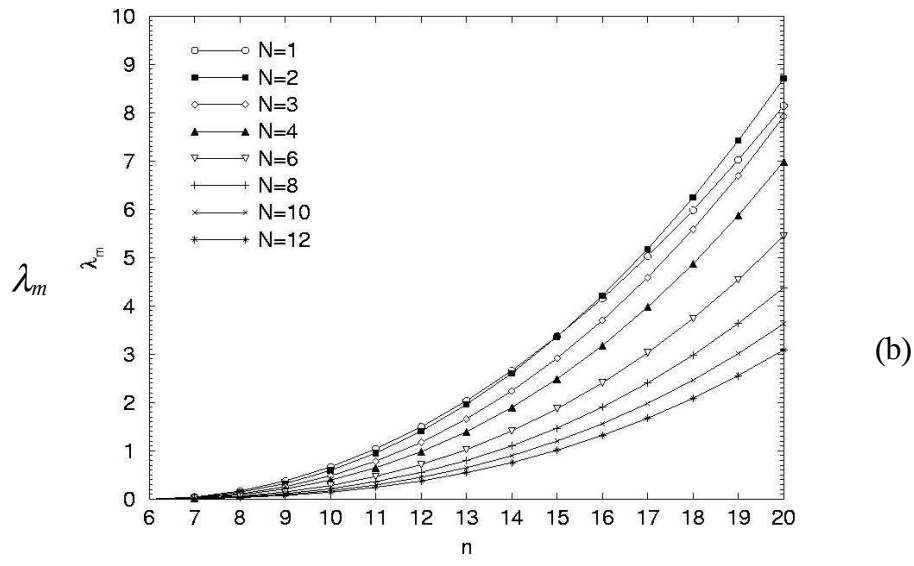
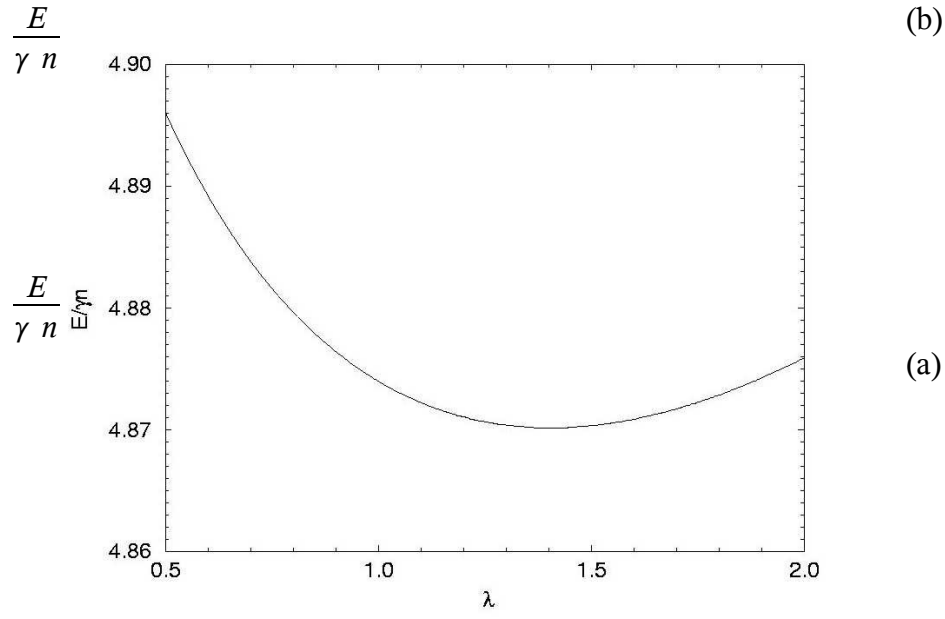


Figure 3

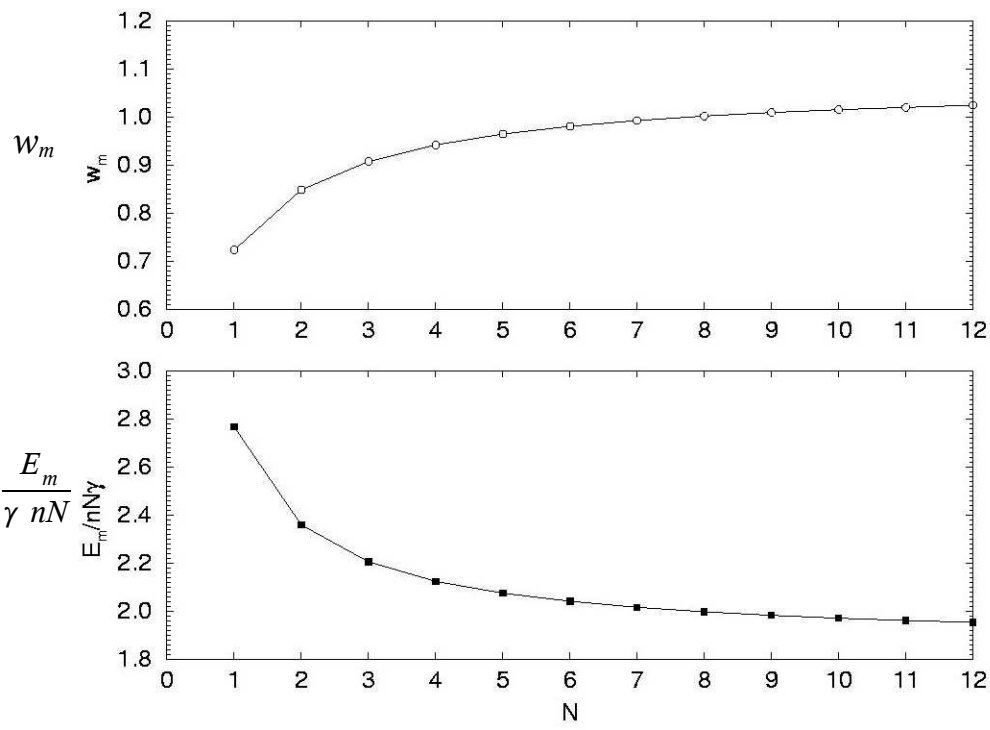
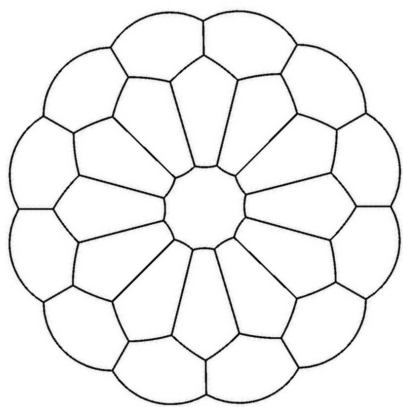
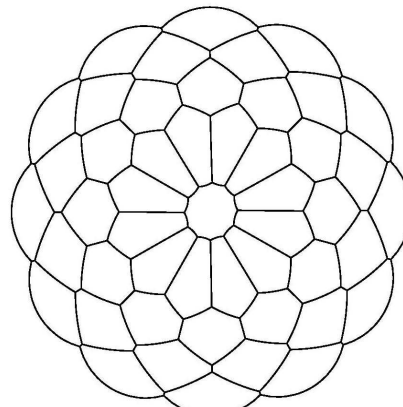


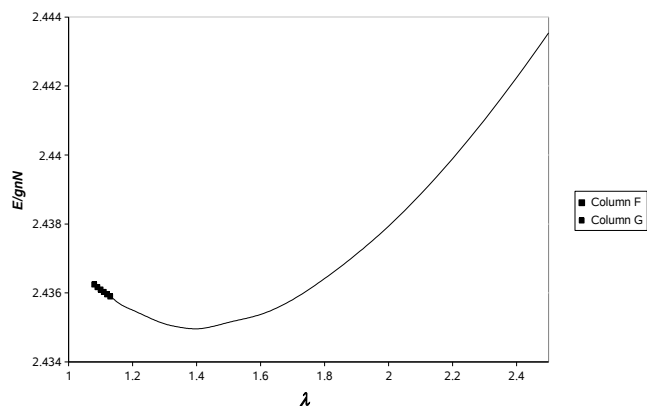
Figure 4



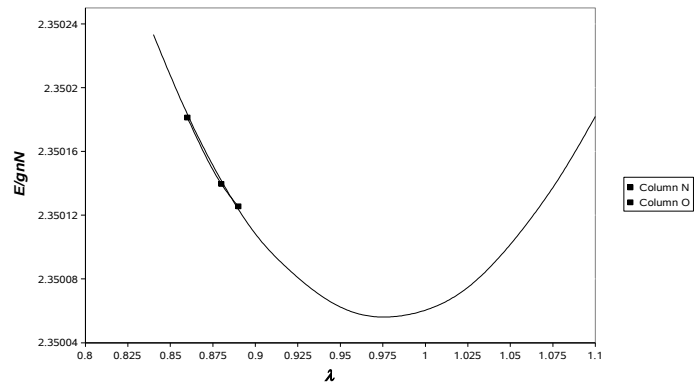
(a)



(b)

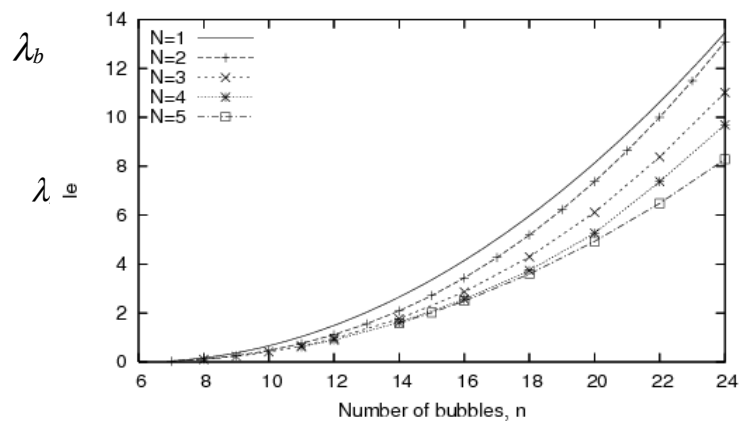


(c)

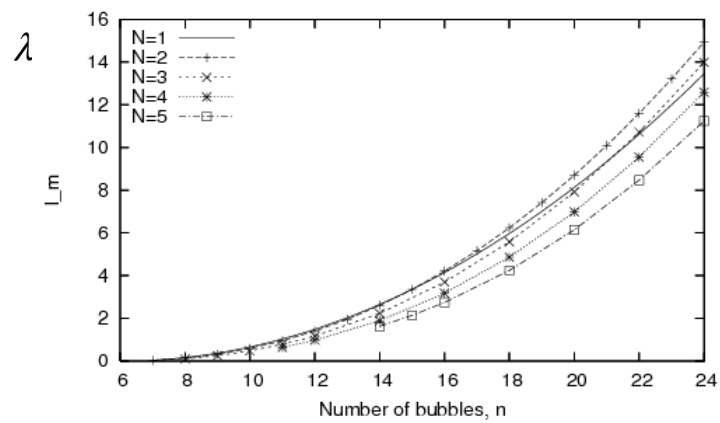


(d)

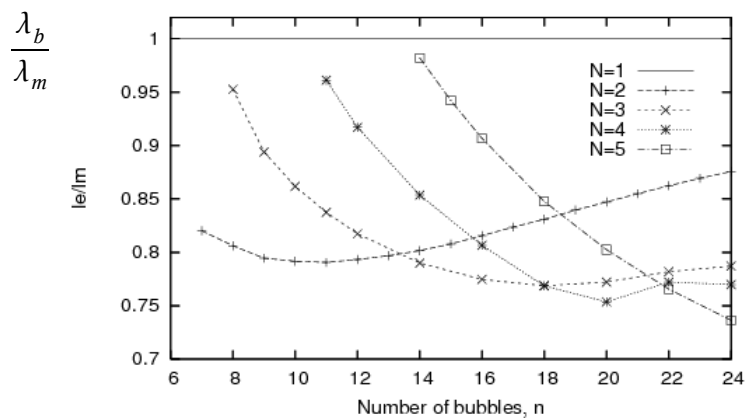
Figure 5 -



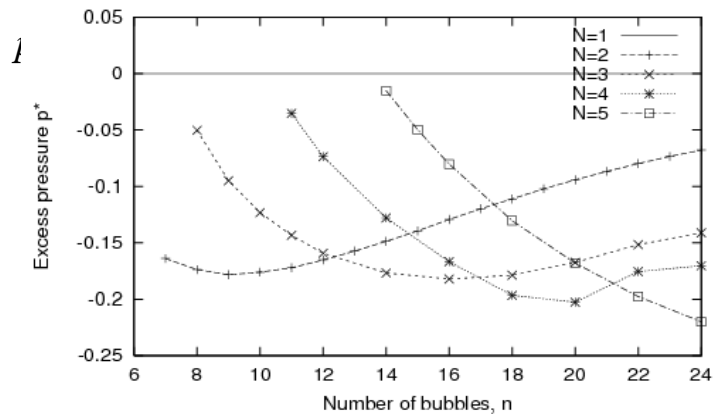
(a)



(b)

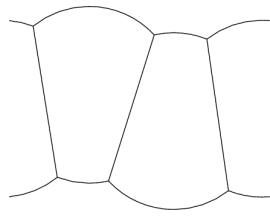


(c)

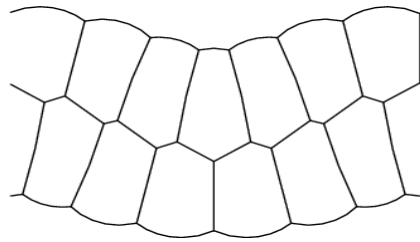


(d)

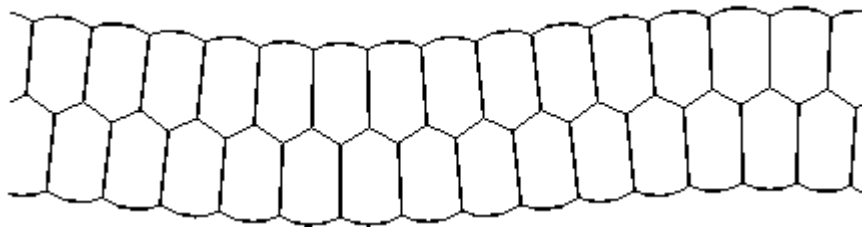
Figure 6



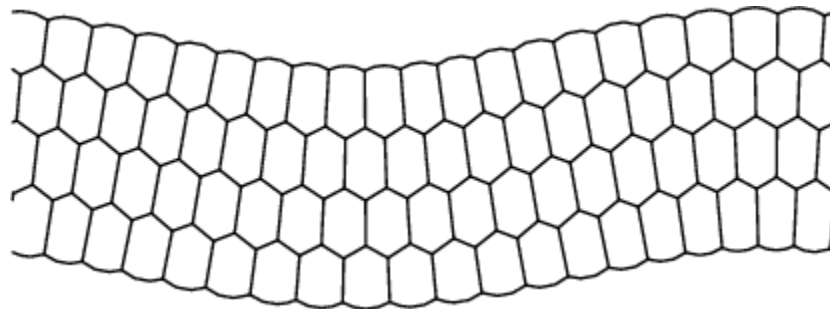
(a)



(b)



(c)



(d)

Figure 7 -

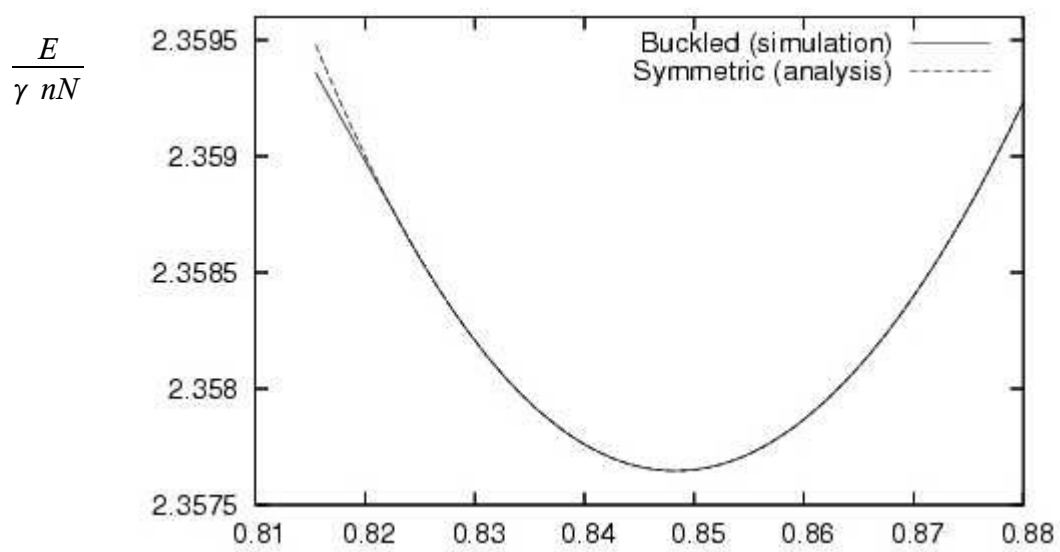
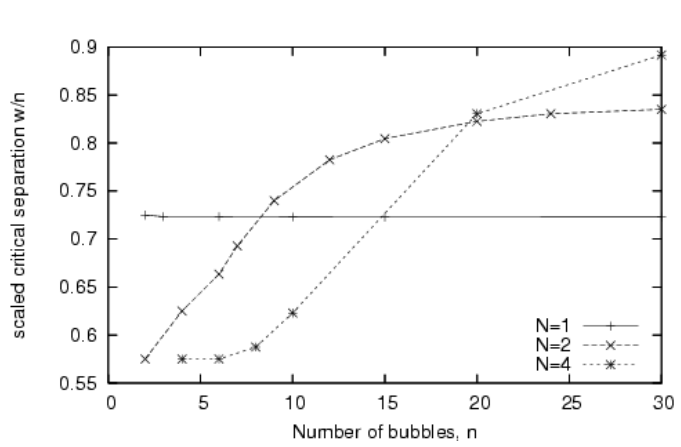
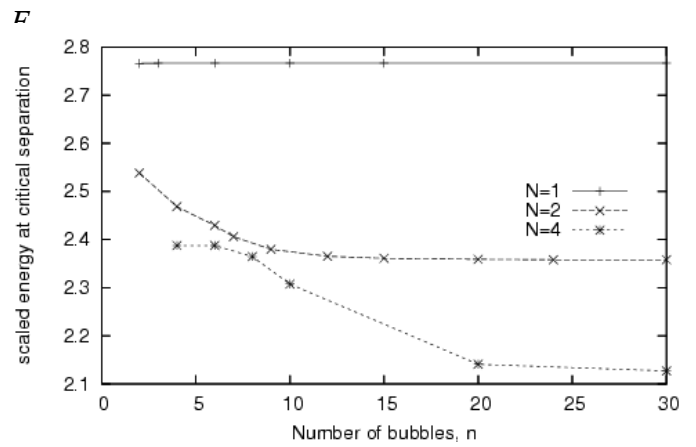


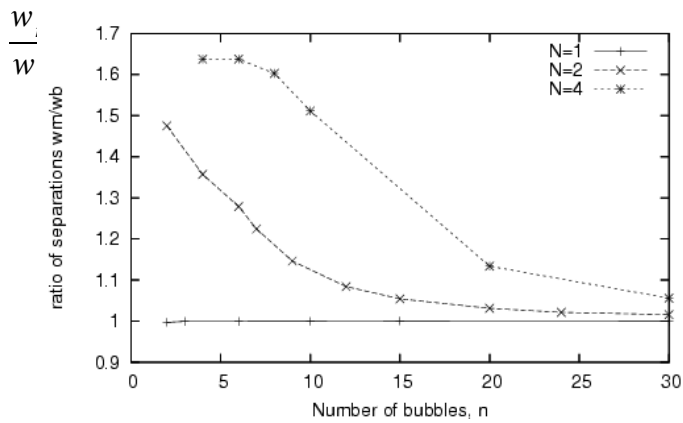
Figure 8 –



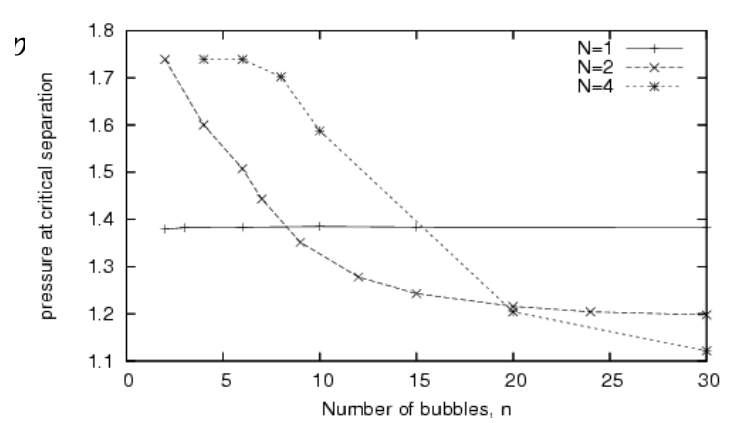
(a)



(b)



(c)



(d)

Figure 9 -

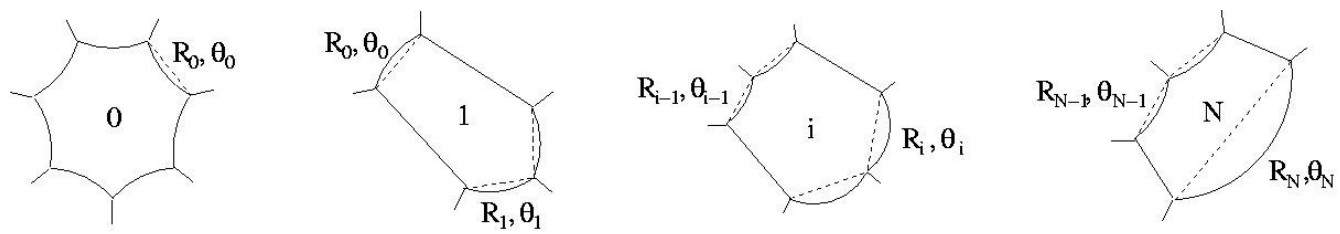


Figure A1 –